

OptiStructures: Fabrication of Room-Scale Interactive Structures with Embedded Fiber Bragg Grating Optical Sensors and Displays

SAIGANESH SWAMINATHAN, Human-Computer Interaction Institute, Carnegie Mellon University

JONATHON FAGERT, Dept. of Civil and Environmental Engineering, Carnegie Mellon University

MICHAEL RIVERA, Human-Computer Interaction Institute, Carnegie Mellon University

ANDREW CAO, Dept. of Civil and Environmental Engineering, Carnegie Mellon University

GIERAD LAPUT, Human-Computer Interaction Institute, Carnegie Mellon University

HAE YOUNG NOH, Dept. of Civil and Environmental Engineering, Stanford University

SCOTT E HUDSON, Human-Computer Interaction Institute, Carnegie Mellon University

A recent topic of considerable interest in the “smart building” community involves building interactive devices using sensors, and rapidly creating these objects using new fabrication methods. However, much of this work has been done at what might be called *hand scale*, with less attention paid to larger objects and structures (at *furniture* or *room scales*) despite the fact that we are very often literally surrounded by such objects. In this work, we present a new set of techniques for creating interactive objects at these scales. We demonstrate fabrication of both input sensors and displays directly into *cast* materials – those formed from a liquid or paste which solidifies in a mold; including, for example: concrete, plaster, polymer resins, and composites.

Through our novel set of sensing and fabrication techniques, we enable human activity recognition at *room scale* and across a variety of materials. Our techniques create objects that appear the same as typical passive objects, but contain internal fiber optics for both input sensing and simple displays. We use a new fabrication device to inject optical fibers into CNC milled molds. *Fiber Bragg Grating* optical sensors configured as very sensitive vibration sensors are embedded in these objects. These require no internal power, can be placed at multiple locations along a single fiber, and can be interrogated from the end of the fiber. We evaluate the performance of our system by creating two full-scale application prototypes: an interactive wall, and an interactive table. With these prototypes, we demonstrate the ability of our system to sense a variety of human activities across eight different users. Our tests show that with suitable materials these sensors can detect and classify both direct interactions (such as tapping) and more subtle vibrations caused by activities such as walking across the floor nearby.

CCS Concepts: • **Human-centered computing** → *Ubiquitous and mobile computing systems and tools*; **Interactive systems and tools**; **Ambient intelligence**.

Additional Key Words and Phrases: embedded sensing, interactive structures, optical fibers

Authors' addresses: Saiganesh Swaminathan, saiganes@cmu.edu, Human-Computer Interaction Institute, Carnegie Mellon University, Pittsburgh, PA; Jonathon Fagert, jfagert@cmu.edu, Dept. of Civil and Environmental Engineering, Carnegie Mellon University, Pittsburgh, PA; Michael Rivera, mlrivera@andrew.cmu.edu, Human-Computer Interaction Institute, Carnegie Mellon University, Pittsburgh, PA; Andrew Cao, ajcao@andrew.cmu.edu, Dept. of Civil and Environmental Engineering, Carnegie Mellon University, Pittsburgh, PA; Gierad Laput, gierad.laput@cs.cmu.edu, Human-Computer Interaction Institute, Carnegie Mellon University, Pittsburgh, PA; Hae Young Noh, noh@stanford.edu, Dept. of Civil and Environmental Engineering, Stanford University, Stanford, CA; Scott E Hudson, scott.hudson@cs.cmu.edu, Human-Computer Interaction Institute, Carnegie Mellon University, Pittsburgh, PA.

Permission to make digital or hard copies of all or part of this work for personal or classroom use is granted without fee provided that copies are not made or distributed for profit or commercial advantage and that copies bear this notice and the full citation on the first page. Copyrights for components of this work owned by others than ACM must be honored. Abstracting with credit is permitted. To copy otherwise, or republish, to post on servers or to redistribute to lists, requires prior specific permission and/or a fee. Request permissions from permissions@acm.org.

© 2020 Association for Computing Machinery.

2474-9567/2020/6-ART50 \$15.00

<https://doi.org/10.1145/3397310>

ACM Reference Format:

Saiganesh Swaminathan, Jonathon Fagert, Michael Rivera, Andrew Cao, Gierad Laput, Hae Young Noh, and Scott E Hudson. 2020. OptiStructures: Fabrication of Room-Scale Interactive Structures with Embedded Fiber Bragg Grating Optical Sensors and Displays. *Proc. ACM Interact. Mob. Wearable Ubiquitous Technol.* 4, 2, Article 50 (June 2020), 21 pages. <https://doi.org/10.1145/3397310>

1 INTRODUCTION

We are surrounded by structures that are purposefully built and provide utility to habitation and living. Structures like walls, tables, beams, etc. span large surface areas and they remain ubiquitous in various walks of life. Most structures serve a useful function of providing and organizing spaces and yet, these structures to date typically remain passive without offering any interactivity or inherent computational abilities. Moreover, the primary goals involved in design and engineering of structures have mainly focused on building and material considerations such as strength, stability, surface characteristics, etc. rather than interactivity or augmentation with computation. As a result, the manufacturing processes for structural components has remained catered towards passiveness.

With the recent advances in computationally-driven manufacturing such as 3D printing [2, 4], printed electronics [59] or hybrid manufacturing (additive + subtractive) [3] we are offered increasing opportunities for designing and manipulating structures from micro to macro scale. Some notable projects such as printed optics [53], metamaterial mechanisms [19, 20], printed composites [49] have utilized such advances for manipulating optical, electrical, and mechanical properties to print multi-functional interactive devices. However, many of these approaches work at what might be called “hand-scale” rather than larger “room-scale” components.

In the work described here, our main goal is to leverage advances in fabrication tools and sensing technology to enable interactivity in the built environments at a larger, and previously less examined, scale. We do this by creating functional structures that are interactive at room scale. To this end, we introduce a computer controlled manufacturing process supporting the construction of cast interactive objects – objects made from a liquid or paste that solidified in a mold. This is supported by a custom modified CNC machine which can both mill custom molds for casting, and insert optical fibers through the surface and within these molds. This process allows ordinary looking objects made from a wide range of cast-able materials to be constructed with interactive capabilities implemented with embedded optical fibers. These optical fibers can both provide input and as well as visual feedback (by delivering light to the surface of the object). Input is implemented using *Fiber Bragg Grating* (FBG) optical sensors which we custom configure into very sensitive vibration sensors. Multiple sensors can be integrated into, or placed in line with, a single optical fiber embedded within an object. Further, they embed only passive components (no electronics) within the material, require no internal power to operate, and can all be interrogated from a single point (the end of the fiber) using a laser-based device. Our tests show these sensors to be extremely sensitive, with an ability to detect and classify both direct interactions such as tapping, knocking, swiping, etc., as well as more subtle actions such as walking nearby or moving a chair across the floor.

Our interactive structures can be manufactured with low-cost, strong, building scale composite materials such as concrete, plaster, polymer resins, composite materials like those used to create faux granite counter tops, bio-fiber composites, etc. These materials are already widely used and readily available in home improvement stores. Our process can be used to manufacture complete objects, or our structures can be post-processed into building blocks or other components, and integrated into existing infrastructure such as walls and living spaces, providing interactivity to our surroundings. Combined together, our manufacturing process, software and hardware pipeline, sensor designs, and machine learning activity classification enable rich interactions with smart infrastructure at a room scale.

Our work makes the following contributions:

- Mold and cast methods for fabricating room-scale interactive structures

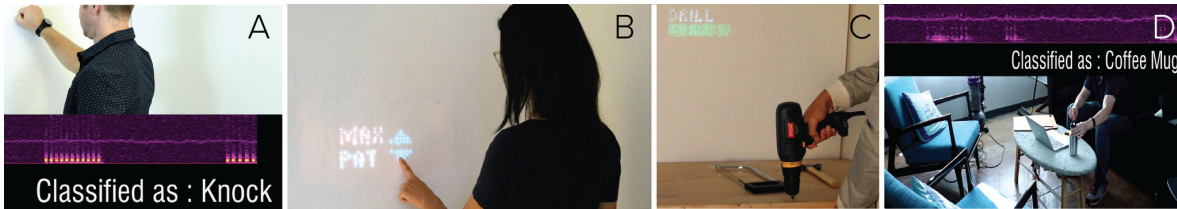


Fig. 1. Embedded fiber optic input sensors and displays can bring interactive capabilities to room scale objects.

- A custom fabrication device for both mold creation and computer controlled fiber optic embedding as needed to support displays and sensors.
- A technique for using embedded fiber-bragg grating optical sensors to detect room-scale activities
- Experimental evaluation of the usable range and configuration of fiber optic sensors
- User validation of various interactions on our fabricated room-scale interactive structure prototypes

In the sections that follow, we will describe our novel fabrication and sensing approach in more detail. First, in Section 2 we give an overview of our fabrication and sensing process. Then, we will consider some relevant prior work in Section 3. This will be followed by sections providing the details of sensing requirements for enabling fabricated interactive structures (Section 4) and the fabrication process itself (Section 5). We will then turn to technical evaluations of the performance our system with respect to casted materials, distance sensitivity, and with respect to other common vibration sensing modalities in Section 7. Next, we evaluate the performance of our with example applications on our two *room scale* prototypes considering a variety of common human activities and across multiple different users in Section 8. Finally, we conclude with discussions and future work.

2 FABRICATION PROCESS OVERVIEW

This section briefly introduces the fabrication and operation concepts which will be described in detail in later sections. Steps for fabrication of interactive structures include: production of a mold, insertion of optical fibers in the mold, and actual casting of materials to form a functional object. The resulting interactive structures can sense human activity/input and provide feedback through visual displays. Each of these aspects is described below.

Production of a mold: Casting of objects is a mature manufacturing approach which can support quite a range of different materials. This flexibility allows our approach to be employed with a wide range of castable materials, provided they: 1) are generally suitable for molding; 2) are compatible with the optical fibers we use (which have a polymer sheath), and 3) provide a sufficiently rigid structure which can propagate vibrations (e.g., cement, plaster, etc., but not soft foams). We demonstrate our approach using a mold created with CNC milling. The final shape is specified in a conventional CAD drawing tool and milled from a block (or a stack of sheets) of mold material using a commercially available ShopBot CNC mill. For convenience and rapid production, the work we present here has used a stiff foam (similar in consistency to Styrofoam) for the molds. However other materials could be used. The primary constraints on mold material are that it must be permeable enough to support optical fiber insertion—done by pressing a stiff fiber through the surface of the mold— and that it must be compatible with the cast material (or coated or covered to make it compatible).

Insertion of optical fibers in a mold: Our approach varies from typical molding techniques in its introduction of optical fibers into the interior, and at the surface of the cast object. We have produced a custom "head" attached to our CNC milling platform which pushes optical fibers (which are fairly stiff) into the surface of our molds. We use 1mm outside diameter optical fibers with plastic cladding, and typical insertion pushes the fibers

4mm into the surface of the mold, while leaving a length of fiber inside the mold. In the final cast object, this will position optical fibers inside the cast object, and protruding 4mm from its surface.

Casting to form a functional object. Once a mold with positioned fibers is produced, casting material is introduced into it by a simple pouring process. Additional fibers with in-line FBG sensors (with an interrogation fiber protruding from the object, as described later) are placed in the middle of the material as it is being poured. After curing, protruding fibers are then typically trimmed to be flush with the surface, and in some cases covered with a surface treatment such as paint.

The optical fibers embedded in the resulting object can serve a dual purpose: 1) they can be configured as highly sensitive vibration sensors through the introduction of Fiber Bragg Gratings (FBGs), and/or 2) with a light source at the end of the fibers, they can be used to generate informational and/or feedback displays.

Sensing for input. One of the novel aspects of the work presented here is the use of Fiber Bragg Gratings (FBGs) optical sensors custom configured as very sensitive vibration sensors to gather user input. FBG sensors have a number of important properties that make them advantageous. FBGs are made out of optical fibers (and as a result physically robust) and require neither a power source of their own nor local electronics inside objects; instead their current value can be read remotely through the attached optical fiber by a laser. Since they are permanently cast within the resulting material, it is advantageous that they are both physically robust and not require a local power source such as a battery. Further, our testing shows that these sensors, when cast into our objects, are extremely sensitive. For example, they are able to detect and classify activities such as walking across the floor near the object, as well as higher intensity vibrations from nearby tool use, and more direct input such as tapping on the object. We explore these advantages as well as other sensing requirements that led to the selection of FBG sensors in Section [section 4](#), and discuss the operating principles and characteristics of these sensors in Section [section 5](#).

Producing visual displays for information and feedback. Similar to work in "transparent concrete"¹, to produce output we generate light at one end of a fiber using an LED or (full color) LED array driven under computer control. This light is then transported by the fiber to its other end at or near the surface of the object to produce a display. We extend this work by introducing a new fabrication device that can insert fibers automatically in specified locations. Since fiber placement is computer controlled, a wide range of displays constructed from dots or diffused dots can be implemented.

3 RELATED WORK

Our work relates to several areas of active research in Civil Engineering and Human-Computer Interaction including structural sensing, large-scale sensing approaches, and fabrication of room-scale structures. In this section, we describe how our work builds on these prior efforts to support fabrication of and interaction with room-scale structures.

3.1 Large-Scale Sensing Approaches

The HCI community has long explored ways to sense interactions on and around objects. These approaches typically examine instrumentation of an object or structure with sensors to support context-aware applications and interactivity.

Single-point sensing methods have shown how to recognize water consumption [13, 14], electrical events on power lines [42], and the location of an individual within a building based on air pressure [41] or electrical noise [48]. More recently, a single plug-and-play device with multiple sensors has been used to detect a variety of activities within a room (*e.g.*, a microwave being used) [32], and when placed in a network of such devices,

¹<https://www.lucem.com/>; <http://www.litracon.hu/en/products>

across multiple rooms [29]. Others have used consumer devices (e.g., a camera phone) to support crowd-sourced answers to context-based questions such as "Are there any parking spots available?" [16, 31].

More generally, human activity recognition has been accomplished with a variety of sensing techniques. Some common approaches include laser vibrometry [56], large surface sensing electronics including inkjet-printed capacitive electrodes and RF antennas [15] off-the-shelf LIDAR sensors [30], microphone-captured acoustic events [11, 28], pressure sensing mats [46], and surface vibration sensing using accelerometers and/or geophones [9, 12, 36, 38, 40, 44].

The current work builds on these prior efforts in large-scale sensing by incorporating an end-to-end, room-scale fabrication pipeline that enables both input and output through embedded optical fibers. Our sensing approach is both low-power and highly sensitive to interactions on and around the fabricated structure. Moreover, a single optical fiber can be instrumented with multiple sensors across larger areas, all while being interrogated at a single point. The optical fibers also serve as an output mechanism that can display context-based information such as when a particular tool is being used in a workshop. As a whole, the current work enables room-scale interactivity via fabrication of functional structures.

3.2 Fabrication of Passive Interactive Room-Scale Structures

A growing number of researchers in HCI community have begun investigating how to enable end-user access to large-scale fabrication processes. One body of work has specifically focused on how users can build passive large-scale structures. For instance, TrussFab [26] introduces a system that enables users to create variations of trusses, print joint connectors and assemble them using plastic bottles as a building material. Similarly, Luo *et al.* [34] built an interactive system that lets users decompose a large-scale 3D objects into smaller parts so that each part fits into the printing volume of a desktop 3D printer. While new printing strategies and computational methods are essential for large-scale fabrication, researchers have also examined how to guide workers in assembling structures via fabricated parts. Yoshida *et al.* [54] proposed a system that uses projection mapping and a hand-held dispenser for chopsticks and glue to build a structure. Similarly, Lafreniere *et al.* [27] proposed an interactive system with a wearable component where a group of workers can be dispatched with tasks to fabricate large-scale structures. Many of these works, however, have focused on end-user fabrication of *passive* structures.

Recent research in large-scale structure fabrication has ventured into supporting interactive applications. For instance, Wall++ [57] demonstrates wall treatment methods and corresponding sensing hardware to turn passive walls into a context-aware structures using electric field sensing of nearby objects. Similarly, Swaminathan *et al.* [50] provide methods to allow end-users to custom fabricate room-scale interactive pneumatic structures. Finally, TrussFormer [25] enables users to create large-scale truss-based structures that actuate. Our work draws inspiration from these projects, but places a greater focus on enabling fabrication of interactive room-scale structures that are made with building-scale materials (*i.e.* concrete, plaster, etc.). Additionally, we show how our fabrication pipeline, embedded displays, and sensing approach create smart infrastructure for room-scale interactivity.

3.3 Structural Health Monitoring

Fiber Bragg Grating (FBG) sensors have been employed for large-scale structural health monitoring (SHM) in civil structures such as dams and bridges [35, 47, 55]. For instance, 26 FBG sensors were placed on a horsetail bridge structure at the intersection between composite wraps over concrete to understand the strength provided by the composite wraps. These sensors were used in preference to conventional (electrical) strain gauges because they can measure several kHz of dynamic strain with a resolution as low as 0.1 microstrain [47]. FBG sensors are also employed for SHM with applications such as monitoring of concrete and engineered wood buildings [10],

composite aircraft wing monitoring [22, 51], and monitoring loads on wind energy turbine blades [8]. For a review of FBG sensors and application in large structures, see Loupos et al [33], as well reviews on work employing FBG sensors for structural health monitoring [7, 21, 24].

4 SENSING REQUIREMENTS

Sensing at room-scale through structures can be enabled by various types of sensors such as a high frame-rate accelerometers, surface microphones, etc. In addition to excellent sensing performance when compared to existing sensors (see Figure 7), our sensing approach offers significant advantages for the design and manufacturing of room-scale interactive structures. Our requirement rationale for FBG sensors is as follows:

R1. Conditions of human use: Typical use of structures is in harsh conditions such as outdoors or floors, pavements, near water, etc. For instance, a concrete counter-top might encounter water splashing from kitchen use or a wall outside might experience rough weather (snow, rain, etc. as well as expansion and contraction of materials) or floors involve the movement of items and constant impact from footsteps. Simplicity and robustness to physical environmental conditions is critical in these settings. Embedding fiber optic sensors is known to work well [17, 58] for such rough conditions, while other powered electronic sensors (such as high FPS accelerometers or microphones, etc.), are sensitive to the presence of water and not as durable for high traffic use. Moreover, in environments like workshops where there is extensive use of power tools, immunity to EM fields is a necessity that FBG offers by being optical.

R2. Cabling Labor: Enabling large-scale interactivity between sections of structures in multiple rooms also requires multiple high FPS accelerometers or other sensors to be placed. However, this requires inordinate amount of cabling labor (if wired) especially if they span across large areas. As seen in aerospace [1], where a single fiber optic cable (with many FBG) has replaced bulky cables and enclosures of traditional sensors (strain gauges) in large-scale structures.

R3. Power: If wireless sensors are deployed (across rooms) they require maintenance by users such as replacing batteries. Whereas we can place multiple FBGs on a single optical fiber and they do not need to be supplied with electrical power. We note that research [18] indicates that sensing can occur on single fibers even as long as 75km without additional amplification. Hence FBG can stay in place for years without requiring any additional power or maintenance.

R4. Design and Manufacturing: Finally, for seamless integration in smart building scenarios, sensors need to be an integral part of the manufactured structure and hidden, rather than things that are configured, attached externally, and exposed. Traditional electronics may not survive embedding during the manufacturing process. For instance, cement begins in a wet and caustic form and undergoes an exothermic reaction during curing, making embedded electronics challenging.

To summarize, we derived our choice of the sensor not only due to their excellent sensing performance, but also as a consequence of the manufacturing process. One that can survive the harsh conditions of use, that can span to large surfaces without requiring power or extra cabling labor, and are immune to EM fields.

5 FIBER BRAGG GRATINGS AS SENSORS

5.1 Theory of Operation

We utilize optical fibers with Bragg gratings for sensing activity and to provide interaction support around our structures. Bragg Gratings are usually located inside an optical fiber and they selectively reflect light at a specific wavelength when presented with a broadband or swept frequency light source (Figure 2). This is done using a series of lines laser etched across the core of the optical fiber at a specific spacing. These lines create variations in the refractive index of the fiber core and result in a wavelength specific dielectric mirror. The *grating period* (distance between the gratings) in these fibers determines the wavelength of the light reflected back. When the

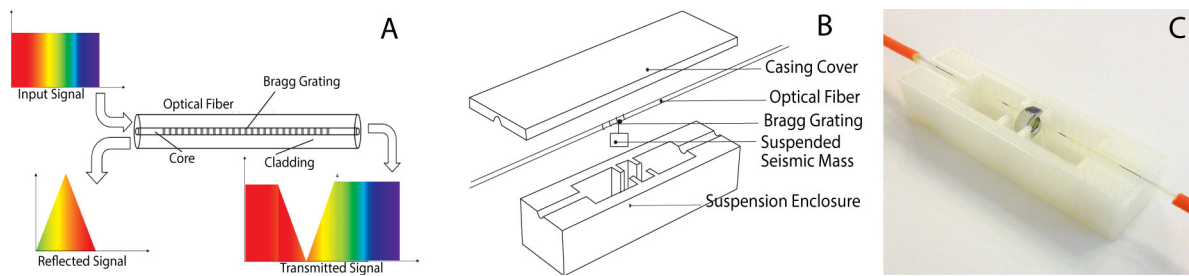


Fig. 2. Fiber-Bragg Grating Optical Sensing and hardware. The Fiber-Bragg Grating Optical Sensor uses bragg gratings on an optical fiber to reflect different amounts of light based on an input signal (A). The input signal is captured on a vibration transducer that houses the optical fiber (B and C).

fiber is minutely stretched (*strained*), this results in a change in the grating period, hence a change in wavelength of the reflected light. By tracking these changes in wavelength, FBGs can sense strain and can be highly sensitive with a gauge factor of 1.2 picometers of wavelength shift per microstrain (or 0.012 microns of wavelength shift per 1% strain).

By using FBGs with different periods many sensors can be multiplexed along a single optical fiber. Since each FBG can have a unique wavelength at which it reflects light, the strain occurring at each FBG can be tracked independently. Theoretically, we can multiplex nearly 100 FBG sensors in single optical fiber extending the sensing range to tens of km with no power required at the sensors themselves. Hence these qualities of the sensor lend well to our purpose of enabling room-scale interactivity.

5.2 Sensing and Interrogation

We use an SM130 Optical Interrogator [37] to sense the wavelength shifts in FBG when subjected to strain. Optical interrogators work by using a swept frequency laser source that passes light into the fibers and then examining the magnitude of reflected light at various frequencies.

FBG's are typically fabricated by using a femtosecond laser source [5]. The machinery to fabricate FBG is expensive, however there are a wide variety of companies which sell ready-made FBGs with pre-defined wavelengths. We use off the shelf FBG fiber costing around \$30 each from Micron Optics [6] and a used laboratory-grade interrogator which costs around \$800. However these devices are relatively simple in nature and with a larger market adoption, the costs of both the FBGs and interrogator could be substantially lower (and low-cost interrogators have already been described in the literature [52]).

5.3 Vibration Transducers

We chose FBG sensors because of their very high sensitivity and resilience to moisture, as well as to the higher temperatures and strain induced during fabrication as part of the curing process of some materials. Typically, FBG sensors are used to monitor strain and temperature for instrumented objects [23], but we have adapted these sensors for use as vibration sensors. By detecting vibration in a highly sensitive way, we can detect (and eventually classify) a range of interactively relevant human actions on or near cast materials.

To convert FBG sensors to vibration transducers we attach a small, known seismic mass (8g) to the fiber optic cable between sets of gratings in the cable. The mass was chosen based on the maximum weight the tensioned fiber can support without tearing apart. We have developed a small 3D printed enclosure box (Figure 2 B and C) to house the fiber-optic sensor and suspended mass. This allows the FBG augmented fibers to pass through either end, with a cavity in the center for placing the suspended mass. By casting the enclosure directly into the material,

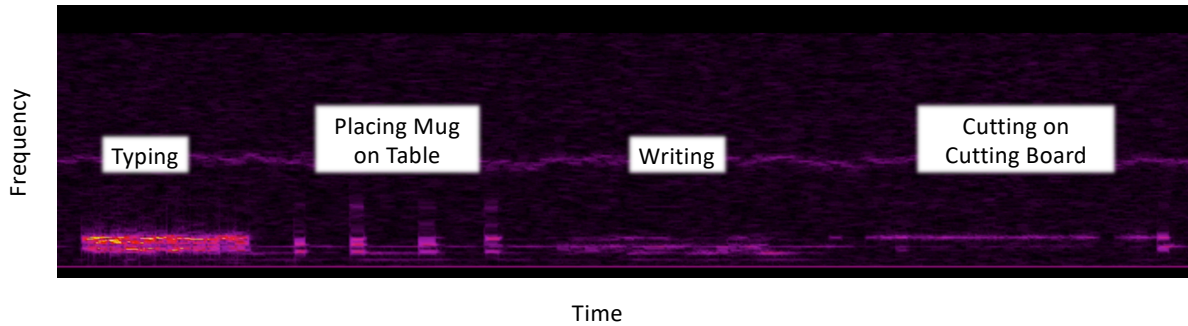


Fig. 3. Spectrogram showing the vibration response variation for different activities on an instrumented table. Color variations represent changes in intensity/magnitude.

we create a bond between the material itself and the enclosure, which ensures that when the material vibrates, these vibrations are reliably transmitted to the seismic mass. When the mass vibrates, it induces a strain in the gratings which is recorded as a change in the wavelength of reflection for the FBGs as seen by the interrogator. This stream of strain values corresponding to vibrations are then used for activity classification.

5.4 Activity Recognition Feature Extraction & Classification

The FBG sensor measures the magnitude of vibrations occurring on the vibration transducer embedded in our cast structure. We sample raw signals at 1kHz, segmented using a sliding window of 512 samples. Next, we apply a Fast Fourier Transform on the windowed signal and we extract features from the resulting spectrum. These features include: the magnitude of each frequency band (in the single-sided spectrum); the first and second derivative of the spectrum; the magnitude for the octave and one-third octave bands; and lastly, statistical measures of the spectral bands (min, max, range, mean, standard deviation, and root-mean-squared).

Figure 3 shows a series of different activities (e.g., typing on a laptop and writing) and their associated raw spectral content. Note the variations in the duration, frequency bands, and amplitudes (intensity of color) for each of the activities. For classification of activities and various user interactions around a cast structure, we use a Support Vector Machine (SMO-SVM, linear kernel) with default parameters (although other models e.g., boosted trees or dense networks are compatible with our sensors). Due to the variations in materials, environmental conditions, and end-use (i.e., applications), we expect that the system will require an initial calibration to train the activity classifier when first installed. Based on our preliminary studies, we have observed that this calibration can be accomplished in just a few minutes.

6 FABRICATING AN INTERACTIVE STRUCTURE

In this section, we consider details of our fabrication approach for creating an interactive structure. The steps of this process are shown for an example object which we will describe later in Figure 4. For this example we made use of a layered mold consisting of a flat base layer (silver) with CNC milled layers stacked over it (Figure 4A). Figure 4B and C show our custom fiber insertion mechanism and the process of inserting fibers in the base layer of the mold. Upon completing injection of display fibers, the mold is filled with concrete (and legs for a table) as well as an FBG sensor to produce the final product (Figure 4D, E, and F, respectively).

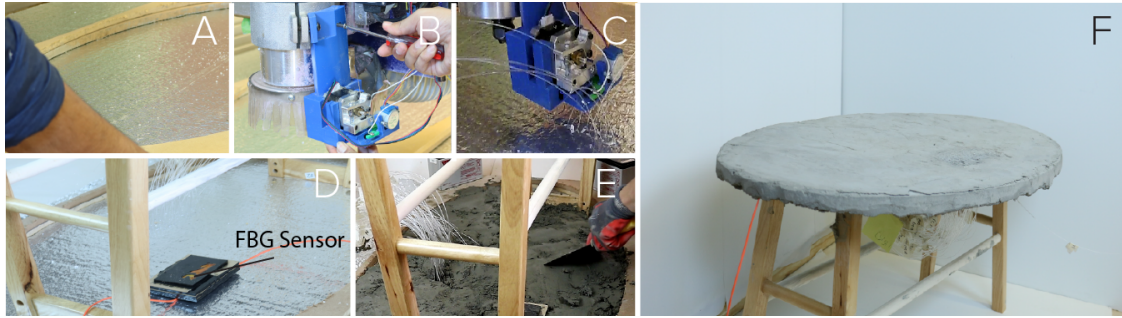


Fig. 4. Fabrication Process for Active Cement Table including milling a mold using a CNC mill (A); attaching the fiber insertion hardware to the mill (B); inserting the optical fibers (C); placing the FBG Sensor (D) into the mold; casting cement into the mold (E); and the finished table (F).

6.1 Fiber Insertion Hardware

As shown in [Figure 5](#), the mechanical design of our custom fiber insertion mechanism consists of a custom-designed 3D printed housing containing two stepper motors. The larger (NEMA17) motor grips the fiber to be inserted with a pinch roller in order to push it into the mold. This drive mechanism is the same as typically used to drive plastic filament into the hot end of a consumer grade FDM 3D printer extruder, and similarly uses an A4988 stepper driver². We use 1mm diameter CHINLY PMMA Optical Fibers³ in our fabrication process. Fiber injection occurs from 4mm above the mold surface and fiber is pushed into the mold at 8mm/s. Typically about 65mm of fiber is left above the injection point to provide a connection point for light insertion.

A second smaller (28BYJ-48) stepper motor (with a ULN2003 driver board) is used to actuate a cutting mechanism using a heated nichrome wire. The motor moves the hot cutting wire forward and back through the inserted fiber using a small rack and pinion mechanism.

6.1.1 Software. To partially support our hardware mechanism, we developed and will make openly available a simple web-based design tool that supports creating fiber optic display inlays on flat mold surfaces as seen in [Figure 5 C](#). The tool allows a user to load a Scalable Vector Graphics (SVG) file, and/or manually draw shapes and patterns. These input shapes are converted to a series of points which fill the shape and can then be used for the hardware's fiber insertion procedure.

The spacing of the fibers can be interactively adjusted to ensure the desired display resolution is obtained before fabrication. Once the desired design is achieved, the user can start the fabrication process via the "Fabricate" button. Our design tool then communicates the point locations to a Python script that performs the fiber insertion procedure using our hardware mechanism (accurately positioned using a ShopBot CNC Machine).

6.1.2 Display Output. The display output of our embedded optical fibers is controlled by an Adafruit 16x32 RGB LED Matrix⁴ that is custom-fitted with a laser-cut mount to hold optical fibers in place. We use an Adafruit Feather M4 Express Microcontroller⁵ with an RGB Matrix FeatherWing⁶ to power and operate the display.

²<https://www.pololu.com/product/1182>

³<https://www.amazon.com/gp/product/B073SML3TY/>

⁴<https://www.adafruit.com/product/420>

⁵<https://www.adafruit.com/product/3857>

⁶<https://www.adafruit.com/product/3036>

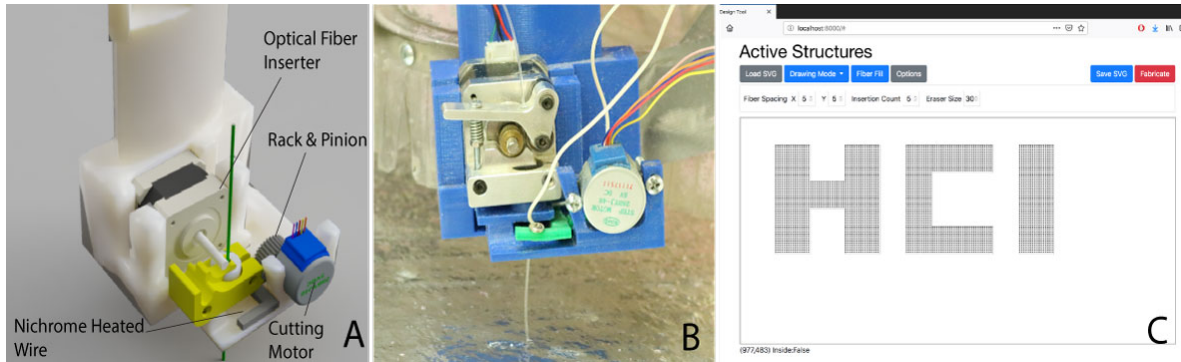


Fig. 5. Optical Fiber Inserter and Cutter Assembly (A), insertion process (B) and design software (C).

7 TECHNICAL EVALUATION

In this section, we describe a series of technical evaluations of our proposed system which explore two primary areas: 1) the sensitivity of various cast materials, and 2) the robustness of our sensing system with respect to distance from the sensing unit.

7.1 Assessing Material Response

To understand the use of embedded sensing and its performance capabilities in different material types, we explored several material types using the fabrication techniques described above. The intent of this study was to 1) determine the sensitivity of our embedded sensing approach in materials of different composition and hardness, and 2) to understand the frequency content of a given activity in different materials as validation for the frequency-based features described above.

To control the inputs to the system, we used a PCB Piezotronics 086D20 ICP impact hammer [43]. In this way, we were able to collect both the input forces/excitations to the system (as readings from the impact hammer), as well as the vibration response from our transducers. This allowed us to normalize measured responses by the magnitude of the hammer strike (and thus directly compare each response). We considered four representative materials for this study: concrete, plaster, hard urethane foam, and soft urethane foam. These materials were chosen because they are common building materials, and because of the variety of material hardness levels that they represent. Further, each test specimen was 0.5 x 0.5m with each material; they were placed each on a flat, horizontal surface and struck it at center with the impact hammer.

For each material, we considered the vibration response from our transducers when the cast sample was struck with the hammer several times. Then, we computed the Fourier transform (FFT) of the vibration response for each hammer strike and found the average frequency response across several consecutive hammer strikes. By considering the average response from several hammer strikes, we reduce the affect of noise and outliers on our material assessment. The average FFT response for each material is shown in Figure 6 A. In these plots, we consider the entire single-sided frequency response of the material due to the impulse from the hammer strike, which are normalized by the magnitude of the hammer strike force. This normalization allows us to study the distribution of frequency content for each material without the influence of varying input magnitude.

From these studies, we can make a few key conclusions about our embedded sensing approach in different materials. First, we can observe that each material has a unique frequency response from the impact hammer, implying that each is responsive to human interactions and these interactions can be sensed with our system. Second, we observe that the frequency content for each material is different; because of this, our system is

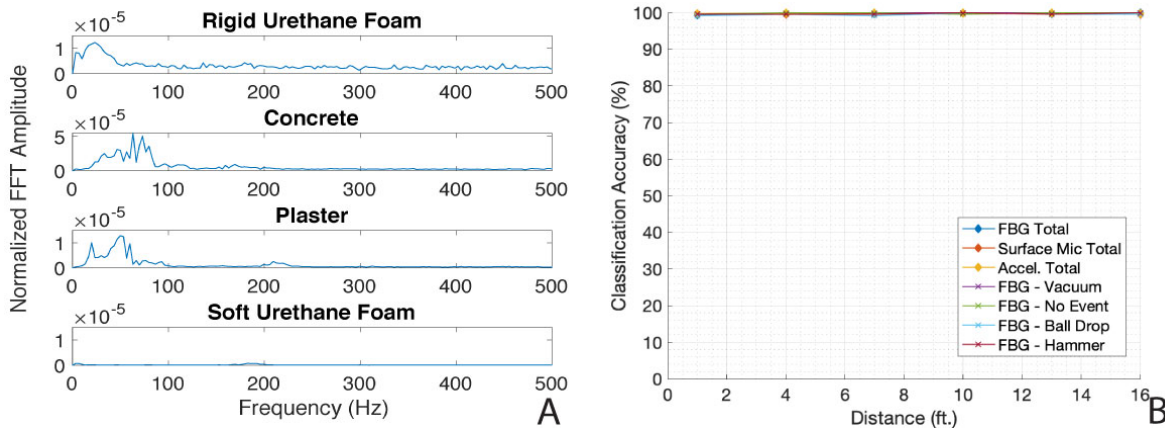


Fig. 6. (A) Frequency responses for different materials subjected to an impulse hammer excitation. Note the changes in frequency content for each material. (B) Shows Combined classification accuracy of our system with varying distance. We observe that with distances of up to 16 ft, there is not an appreciable decrease in performance of our system.

sensitive to the material being used and should be calibrated for each application. Third, the frequency content is widely distributed across the range of frequencies, indicating that our approach (which uses the entire frequency spectrum for features) is appropriate for identifying and classifying human interactions with the cast surfaces. Lastly, the “soft foam” raw signal and frequency spectrum response from the impact hammer has a very low signal-to-noise ratio and was difficult to identify from the ambient vibration signal. As a result, we can conclude that while we could identify the hammer strike, soft materials such as the one tested may not be appropriate for less impulsive or lower intensity interactions.

7.2 Distance Studies

In addition to the material tests, we explored the sensitivity of our approach and sensing system to estimating activities with varying distance from the sensor. To accomplish this, we deployed our sensing system in a large open area on a wooden gymnasium floor and performed a series of three activities at increasing distances from the sensor (3 ft. increments starting at 1ft.). The FBG sensor along with the enclosure was placed directly on top of the wood floor and fastened with a high-strength fiber tape to create a strong coupling with the floor structure. This coupling ensures that human activity-induced floor vibrations are transmitted to our sensors with as little loss of information as possible. In a long-term deployment, we anticipate that the sensors could be cast directly into the floor structure or a casted wood panel could be placed in a floor opening and fastened to the adjacent flooring members.

The activities we considered were: 1) a series of ball drops from knee height, 2) running a vacuum on the floor, 3) a series of hammer strikes on the floor, and 4) no event (i.e. no human interaction with the floor). For each activity we collected approximately 300 samples of vibration data for each activity and used this data to train and evaluate our activity recognition classifier. We evaluated each discrete distances (1, 4, 7, 10, 13, 16 feet) independently with a 10-fold cross validation and determined the accuracy at each distance by computing the total number of correctly classified instances divided by the total number of instances. Figure 6b shows the results of our study. From these results, we observe that the accuracy of our approach is very high ($> 99\%$) and approximately equal across all distances. Further, this performance is consistent across each activity, with each class having similar performance ($> 99\%$ accuracy) at each distance. This indicates that our system is robust to

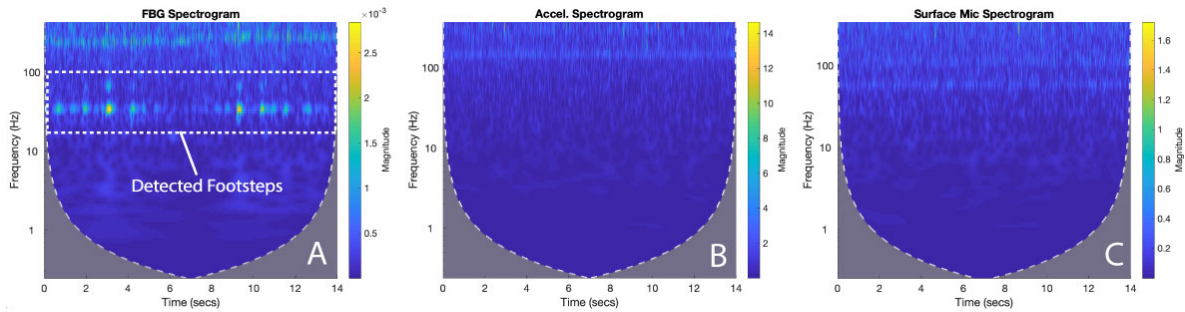


Fig. 7. Spectrogram showing the footstep detection at a distance of 16 feet for three sensors – FBG (A), accelerometer (B) and surface microphone (C). Note that the FBG can clearly detect many of the footsteps, while there is no visible response from the other two sensors.

distance from the sensing unit, and is capable of distinguishing activities through and across a floor at distances as great as 16ft.

Study 1: To compare the performance of the FBG sensors with other common sensing modalities, we collected the same distance study data with a surface microphone (TIMESETL Piezo Contact Microphone) and an accelerometer (ADXL345). To ensure there was no bias due to variation in performing each activity, the data for each sensor was collected in parallel (i.e., all three sensors collected data from the same activity simultaneously) and used the same activity classification framework. The results for this sensor comparison are shown in Figure 6 B). As can be seen in this figure, the FBG sensors achieved the same level of overall performance as the surface microphone and accelerometer (> 99% total accuracy for each sensing modality for each distance). Based on these results, we can conclude that the FBG sensors have similar sensing capability as the two common vibration sensors considered upto 16ft, and is well-suited to sensing various human activities across many different distances from the sensor itself.

Study 2: The activities considered in the previous study primarily represented only highly impulsive (e.g., ball drop, hammer), or high frequency (vacuum) excitations. To explore the performance for lower amplitude and lower frequency excitation, we considered the ability of each sensor to detect footsteps at a distance of 16ft. The experimenter walked across laterally at 16 feet mark from the sensors. There were 20 steps in total, 10 steps one way, turn around and walk another 10 steps. Our results (shown in Figure 7) indicate that FBG are can detect most (>15) of these footsteps while other sensors fail to see any activity. This demonstrates the sensitivity of FBG sensors for subtle human activity such as walking at room-scale (16 feet) and their promising use if integrated into structures.

8 APPLICATIONS

We fabricated two prototypes—an *Active Wall* and an *Active Cement Table*—to demonstrate our fabrication technique. In this section, we describe these room-scale structures and how they enable a series of interactive applications such as an environmentally-responsive contact directory, a passive workshop activity display, and a music player controlled with surface gestures.

8.1 Active Wall

Our *Active Wall* consists of a cast rigid urethane⁷ structure with embedded display and sensor optical fibers. The fabrication process is shown in Figure 8. For this example we designed and injected a rectangular matrix

⁷<https://www.alumilite.com/Shared/PDF/Amazing-Casting-Resin-Alumilite-White-TDS.pdf>

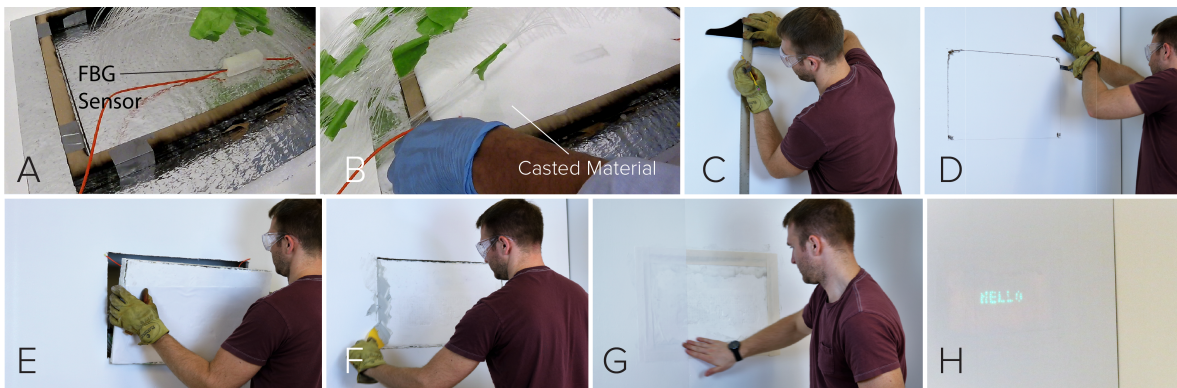


Fig. 8. Fabrication Process for Active Wall. A FBG sensor is placed into a rectangular mold containing an injected fiber optic display (A). Material is cast into the mold (B). A region of an existing dry wall is removed and replaced with the cast structure (C-G). Finally, the display output of the optical fibers is tested and reveals the message "Hello" on the wall (H).

of optical display fibers for display. Note that for this prototype of our system, the optical fibers for the display were independent of those used for sensing (FBG sensor), hence can function simultaneously without issues. After placing the optical fiber sensor, we cast the rigid urethane into the mold and let it cure. We measured the structure and removed its dimensions from a pre-existing sheet of dry wall. Lastly, we placed the structure into the wall and finished the surface with joint compound and a uniform contact paper. Figure 8H shows the embedded optical fibers activated, displaying the word "Hello".

The Active Wall supports a number of surface-based gestures including swipe, knock, and taps localized to particular areas of the wall (Figure 9). The wall is also able to detect events in the environment such as a person walking up to the wall or a power-tool (e.g., hand drill) being used nearby. We leverage these interactions with and around the wall to create an interactive contact directory and passive workshop activity display.

8.1.1 Interactive Contact Directory. Our interactive contact directory (Figure 10A-D) initially begins in an off-state to conserve energy that is typically consumed by other always-on displays. As a user approaches the wall, the vibrations from her walk trigger a welcome message to appear on the display. The user can then use different surface gestures to interact with the wall. A swipe gesture dismisses the welcome message and shows the full contact directory. Tapping near the various touch regions (i.e. the up / down arrows of the directory) allows the user to scroll through the list. A knock gesture selects a highlighted contact to reveal which direction the user should go to find the selected contact.

8.1.2 Passive Workshop Activity Display. Maker-spaces and lab environments have a variety of tools and equipment that create unique vibration patterns. As another application, our active wall can recognize when these tools are being used and display the magnitude of the vibrations via the wall's embedded optical sensor and display (Figure 10 E-G). If another user enters the workshop area while a dangerous tool (e.g., a saw) is being operated, the wall triggers a context-aware safety alert (Figure 10 H). Finally, detection of these workshop activities can be used to log tool usage over time, supporting automated maintenance reminders, and to let other users know when a particular piece of equipment (e.g., laser cutter) is available for use. .

8.1.3 Active Wall Activity Recognition Evaluation. We conducted three studies with our smart wall prototype: 1) a gesture study with multiple users to evaluate the ability of our system to distinguish wall interactions, 2) a localization study where multiple users interacted with the wall in different locations to determine the spatial



Fig. 9. A variety of surface gestures such as a knock (A), tap (B) and swipe (C) can be reliably detected in discrete locations as seen in their respective spectrograms.

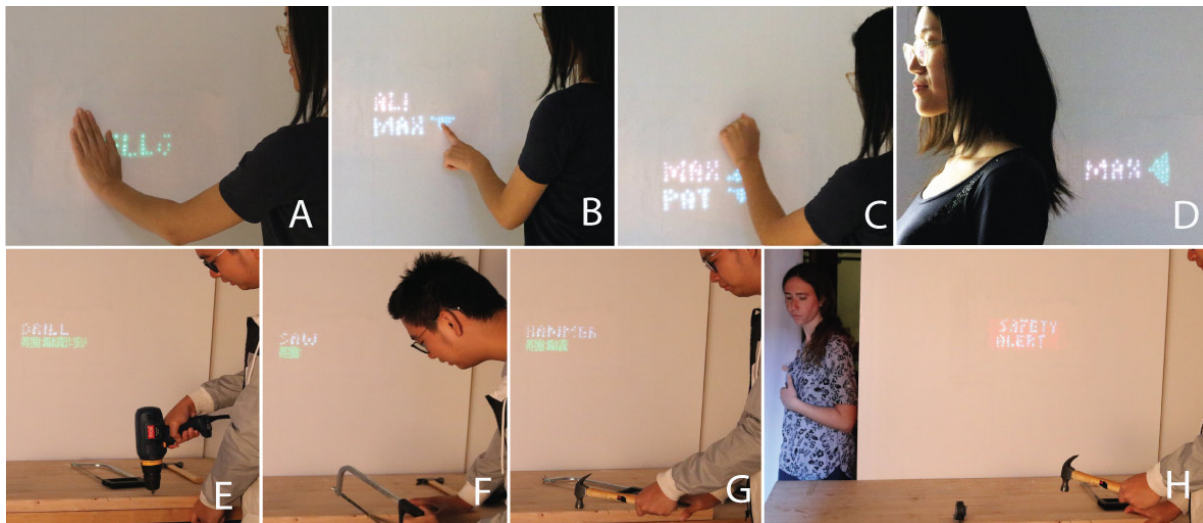


Fig. 10. Applications of the Active Wall. An interactive contact directory application uses gesture input and visual feedback to guide users to where they need to go (A-D). A passive workshop activity recognition application senses what tools are being used (E-G) and warns users when another person enters the shop area to enhance workshop safety (H).

sensitivity of the active wall, and 3) a workshop activity study with multiple users where we explore how well the active wall can sense and distinguish activities occurring in the surrounding environment. All user studies were conducted in accordance with an approved IRB Protocol.

Study 1: Gesture Classification Accuracy

Procedure: In our gesture study, we asked a total of 8 experimental participants to interact with our prototype wall using a series of three gestures: tap, knock, and swipe. The experimental participants age range is approximately 21-33 and there were 7 men and 1 woman. We selected the three gestures above as they are among the most common and familiar ways to interact with a surface. For each gesture and each user, a total of approximately 300 samples were recorded. We also collected an additional 300 samples of ambient conditions to train a null state (*i.e.* 'No Event'). Once completed, the data collected from each user was pooled into one dataset and analyzed using the SVM classifier described above and a 10-fold cross validation to assess the overall performance of our system.

Actual	Predicted			
	Knock	Tap	Swipe	No Event
Knock	89.7	6.1	3.6	0.5
Tap	6.0	86.9	6.3	0.7
Swipe	2.4	6.7	86.4	4.6
No Event	0.4	0.8	2.9	95.9

Actual	Predicted								
	Loc1	Loc2	Loc3	Loc4	Loc5	Loc6	Loc7	Loc8	No Event
Loc1	83.6	1.4	2.1	2.4	3.6	1.2	2.5	2.0	1.2
Loc2	1.8	81.3	5.9	1.8	1.6	3.0	2.4	2.0	0.3
Loc3	3.9	7.5	67.1	5.6	2.6	3.5	6.2	3.1	0.5
Loc4	5.1	2.5	4.5	69.9	3.1	2.2	4.4	7.3	1.0
Loc5	6.1	1.5	1.9	2.7	72.8	5.3	5.8	3.0	0.9
Loc6	2.9	4.6	2.8	1.5	3.6	72.3	8.2	3.0	1.1
Loc7	4.1	2.6	3.6	3.0	3.7	6.0	71.0	5.5	0.6
Loc8	2.6	0.7	1.6	4.0	1.8	0.6	2.9	84.7	1.1
No Event	0.6	0.0	0.0	0.2	0.2	0.0	0.1	0.7	98.2

Fig. 11. Active wall classification accuracy for gestures in user studies with 8 participants. The left confusion matrix shows performance of the prototype in identifying common wall gestures (knock, tap, and swipe) across 8 participants. The right confusion matrix shows performance of the active wall in identifying tap locations across 8 participants.

Results: We compute the accuracy of our system for the gesture study as the combined results from the 8 users. The resulting classification accuracy is presented using a confusion matrix in Figure 11. In this figure, darker green colored cells represent higher accuracy, while darker red cells represent higher error. Each of the 4 classes (the three gestures and 'no event') achieve high accuracy with few instances of false predictions. The total classification accuracy across all classes is 89.7%. We note that the highest accuracy is from the 'no event' class, which indicates that our approach is able to determine that someone is interacting with the wall with high accuracy. These results indicate that our approach is robust to varying input styles (*i.e.* those from different users), and can accurately determine the type of input; which enables gesture controls for various applications.

Study 2: Gesture Location Resolution

Procedure: In this study, we asked the same 8 users described above to conduct a series of taps at predefined locations on the active wall. The goal of this study is to understand the resolution of the gesture activity recognition and to showcase the ability of our system to identify the location of the wall interaction. The intuition behind this ability of our system is that interactions in different locations generate unique vibration signatures due to spatial variations in the material itself (*e.g.*, relative position with respect to boundary conditions), and/or amplitude variations due to distance-based signal attenuation. As a result, our system can learn these variations and identify the location of the interaction. The interaction area for this study was a 2ft wide x 1ft tall section of the wall divided into a 6in x 6in grid for a total of 8 tap locations. The "tap locations" represent the center of each grid, and were numbered sequentially along rows, with numbers increasing left-to-right and top-to-bottom. Users were asked to tap in the center of each location in sequence and a total of approximately 300 samples were recorded for each person and for each tap location. The data collected from each user was pooled into one dataset and analyzed using the SVM classifier with a goal of predicting the correct tap location. As before, we used a 10-fold cross validation in our analysis of this dataset.

Results: Figure 11 presents results from this study. The total classification accuracy for this study was 77.9%, with the best performance at Locations 1, 2, and 8. Locations 3 and 4 are the worst performers, each with an accuracy less than 70%. Of note is that 'no event' has a 98.2% accuracy, which indicates that our approach can detect a tap gesture in almost all cases (*i.e.* very few missed interactions). Overall, the results from the gesture location study indicate that there is potential for our system to locate where a user is interacting with the wall, but it has limitations across multiple users. The cause of this observed performance may be due to the variations in how each user taps on the wall. Some users may have a longer duration or different intensity with taps in each location, which may cause confusion in the model at different locations. In our future work we plan to address

Actual \ Predicted	Cutting	Typing	Vacuum	Chair	No Event	Writing	Coffee Mug
Cutting	85.1	3.5	0.0	0.6	0.4	7.3	3.0
Typing	5.8	88.2	0.3	0.6	0.2	3.9	1.1
Vacuum	0.1	0.3	99.1	0.3	0.0	0.0	0.0
Chair	0.8	0.6	0.0	95.8	1.9	0.2	0.6
No Event	0.7	0.1	0.0	2.7	96.0	0.0	0.6
Writing	10.4	5.8	0.0	1.1	0.2	79.7	2.8
Coffee Mug	4.2	2.1	0.2	1.5	2.1	3.5	86.5

Actual \ Predicted	Walking	Hammer	Drill Press	CNC Vacuum	No Event	Hand Sander	Door Open/Cl	Miter Saw	Laser Cutter
Walking	91.1	1.0	0.6	1.0	0.7	1.7	1.9	1.4	0.5
Hammer	1.3	96.8	0.1	0.8	0.0	0.0	0.4	0.3	0.2
Drill Press	0.4	0.2	97.5	1.5	0.0	0.0	0.1	0.2	0.0
CNC Vacuum	3.6	1.4	1.6	88.3	0.7	0.9	1.0	0.6	2.0
No Event	1.5	0.0	0.0	0.5	84.6	7.3	4.4	0.0	1.8
Hand Sander	1.6	0.1	0.0	0.5	7.2	82.9	5.2	0.1	2.4
Door Open/Close	2.9	0.6	0.0	1.1	5.0	5.5	81.8	0.0	3.0
Miter Saw	3.4	0.7	0.1	0.8	0.0	0.3	0.1	94.6	0.1
Laser Cutter	0.5	0.2	0.0	2.2	1.9	4.7	2.6	0.1	87.9

Fig. 12. Confusion matrices for various events on two interactive structures. (A) shows performance of embedded coffee table unit in identifying various activities. (B) shows performance of the active wall in identifying various shop activities.

this limitation by incorporating multiple sensors into the active wall. With multiple sensors, we can combine the classification data with relative amplitude data (interactions closer to a sensor will generate higher amplitude) and/or time difference of arrival information (which has been shown in prior work to be effective for localization with human-induced vibration signals [39, 40]) to improve the localization capabilities of our system.

Study 3: Workshop Activity Identification

Procedure: In the final study for our active wall prototype, we explored the performance of our system with respect to activities that occur in the surrounding environment. Therefore, we conducted a series of activities in the space surrounding our prototype wall to simulate a “workshop”. The activities studied include (approx. distance from sensor in parentheses): using a table saw (15ft.), walking around the workshop (~5ft.), using a hammer on a table (12ft.), running a miter saw (7ft.), opening/closing a shop door (32ft.), operating a drill press (8ft.), operating a laser cutter (32ft.), using a hand sander (12ft.), running the vacuum system for our CNC router (8ft.), and ‘no event’. These activities were chosen as being representative of common tools/activities that would take place in a normal workshop environment. The distances described in the workshop study reflect the actual location for each tool/activity from the location of the sensor/wall. These locations, therefore, reflect a real-world workshop layout and not one that was tailored for best performance of our system. Our experimental dataset for this study consisted of 8 total users with approximately 300 samples per person and per activity, for a total of approximately 21,000 samples. We computed the total classification accuracy for each event across all users with a 10-fold cross validation.

Results: Figure 12 b) presents a confusion matrix for this study. We observe that the best performance is in identifying operation of the drill press, hammer, and miter saw (97.5%, 96.8%, and 94.6% accuracy, respectively). We note that these particular activities are either 1) very close to the wall, and/or 2) have very high intensity vibrations. As a result, the recorded signals are very distinctive and our system is able to identify these activities with very high accuracy. Further, the worst performing activity is ‘Door Open/Close’, which primarily gets confused with the the hand sander and ‘no event’ activities. In this case, the door open/close is very far from the sensor; as a result, the recorded vibration signal is of very low amplitude and the vibration frequency content is similar, making it difficult to distinguish it from the ambient vibration condition (no event). Overall, the average classification accuracy across all activities is 89.4%, which indicates that our system is able to accurately identify indirect activities in the surrounding environment.

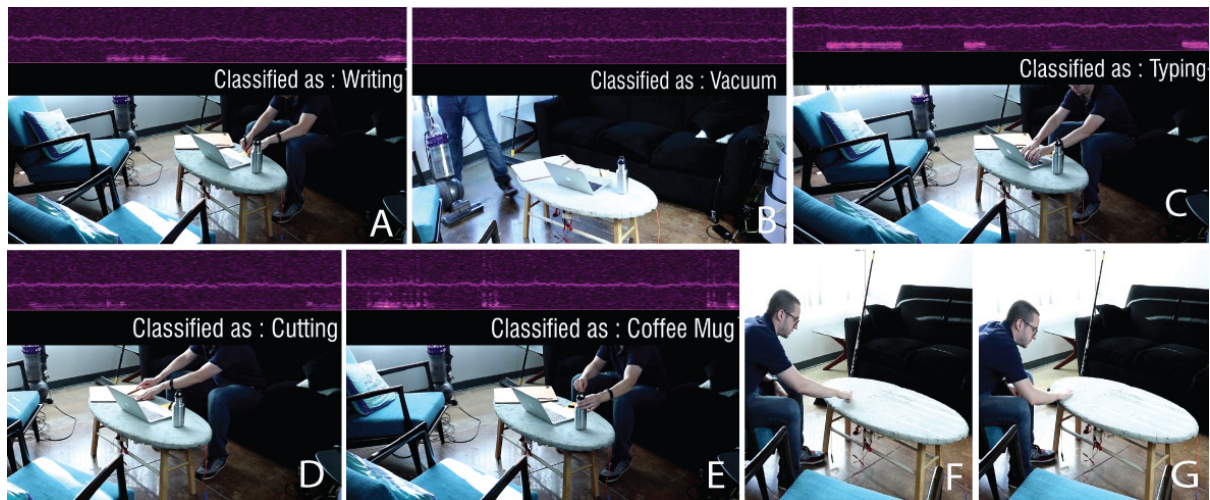


Fig. 13. Applications of the active table including activity recognition of interactions on and around the table (A-E) and a gesture based music player that uses tap, swipe, and knock. as input control for a music player.

8.2 Active Cement Table

We fabricated an Active Cement Table with embedded optical fibers and a sensor using polymer-modified, rapidly curing structural concrete⁸ as seen in Figure 4. We created a mold using the CNC mill, then used our fabrication process to insert a rectangular matrix of optical fibers. After manually placing an enclosed sensor and wooden support legs for the table, we poured and smoothed the concrete and allowed it to cure.

Similar to the Active Wall, our table can detect knocking, swiping and tapping on its surface. Additionally, the table can detect other surface-based interactions common to its typical use in home or coffee shop. For example, the table can sense when a user is writing a note, typing on their laptop, or placing their coffee mug down. Activities in the environment such as a vacuum running or a person sweeping the floor are also detectable. Figure 13 shows an example of some activities measured on/around the active table and their associated spectral responses (which are used for classification).

8.2.1 Surface Gesture Music Player. Our Active Cement Table functions as a gesture-controlled music player. When the user knocks on the surface of the table, music begins to play. A swipe gesture then advances to the next track of a playlist. Finally, knocking again turns the music off. An example of this application is shown in Figure 13 F-G.

8.2.2 Around Table Activity Awareness. Sensing activities around the table enable a variety of context-aware applications. When a user begins to vacuum the floor, their music can be automatically paused for the duration vacuuming. The music can then be resumed once the vacuuming is completed.

8.3 Active Cement Table Evaluation

To evaluate the performance of our active cement table prototype, we conducted an activity recognition study which incorporates activities occurring both on and around the active table.

⁸<https://www.amazon.com/dp/B078753CQW>

Procedure: For this study, we had 8 users conduct a series of activities on the active table prototype, and then in the surrounding environment. This combination of activities enables us to evaluate the performance of our system with regards to horizontal surfaces, and with room-scale activity recognition. The activities on the active table include: typing on a keyboard, placing a mug on the table, writing on a notepad on the table, and using a knife to chop food on the table (e.g., an apple). Then, for activities surrounding the table, we considered the following: vacuuming the floor, and sliding a chair into/out of the table area. Similar to the active wall evaluation, we collected approximately 300 samples of each activity across 8 different users (approx. 16,000 total data samples) and analyzed our system’s classification accuracy using a 10-fold cross validation.

Results: Using our approach, we were able to classify 7 activities (6 listed above and ‘no event’) with a total classification accuracy of 90.1% for our multi-user recognizer. The full results are presented in Figure 12 A. From these results, we can observe that the best performing activity is the vacuum (99.1%), while the worst is writing (79.7%). We note that the writing activity is typically of low intensity, which can lead to confusion with other table activities (i.e., cutting and typing). With its accurate performance across activities both on vertical (active wall) and horizontal (active table) surfaces, we demonstrate that our system is capable of sensing room-scale activities with multiple users.

9 DISCUSSION, LIMITATIONS, & FUTURE WORK

9.1 Sensing of Simultaneous Activities and Interactions

We have leveraged machine learning to sense different interactions on and around our interactive Structures. In our technical evaluation, we focused on sensing events independently. However, as future work it may be advantageous to support classification of simultaneous events. For this purpose, we are interested in exploring a multi-level SVM classification approach similar to [32, 45] and using a network of sensors as in [29] to detect simultaneous events with our system.

9.2 Building-Scale Sensing Infrastructure

Current work demonstrates the feasibility of our sensing approach being integrated into existing infrastructure and/ while building new structures. In future, we aim to scale our approach across different sections of a full-scale building such as walls, floors, etc. by combining multiple FBG spread across different rooms and floors, all while connected through single mode optical fibers⁹ which are interrogated from a single point. Compared to traditional approaches (i.e., wireless sensors/wired sensors), this approach could offer battery and electronics-free sensing at building scale.

Additionally, a practical way to scale FBG sensing into buildings or cities may be to combine them with already existing optical fiber networks for internet/intranet communications. For instance, google fiber¹⁰ offers services by extensively reworking public and private infrastructure with optical fiber networks. By utilizing such intricate optical network may be one way forward to scale sensing approach to building/city scale.

9.3 Material Selection for Interactive Structures

The cast material’s curing process should be considered when incorporating FBG sensors into structures. In general, the FBG sensor functioned correctly in the various materials we had cast around it. However, we found poured concrete requires one additional consideration– concrete cures through an exothermic reaction. In our initial experiments, we found the vibration transducer enclosure (3D printed with PLA) would deform slightly under the heat, affecting the signal response. To address this during fabrication, we coated the enclosure in a

⁹<https://www.cablewholesale.com/specs/10f2-006nh.php>

¹⁰<https://support.google.com/fiber/answer/6124985?hl=en>

high-temperature epoxy¹¹. This issue could also be resolved by fabricating the enclosure with a high-temperature resistant plastic or ceramic material.

10 CONCLUSION

Our work demonstrates a fabrication approach to embedding input and output into the construction of room-scale objects using optical fibers and Fiber Bragg Grating optical sensors. We show through technical evaluations the robustness of FBG sensors with respect to embedded material type and activity distance and compare the performance of our system with common sensing modalities. To showcase the ability of our system to monitor human activity, we evaluated its accuracy across two real-world prototypes with 8 different users and observed a high classification accuracy as much as 89.4% across as many as 9 different activities. Our technique enables a rich application space for interactions occurring on and around these structures. Mark Weiser once stated that the most profound technologies disappear by weaving themselves into the fabric of everyday life. We view our work as a literal building block towards this vision of Ubiquitous Computing by enabling HCI researchers and practitioners to explore interaction with smart structures in big way.

ACKNOWLEDGMENTS

We would like to acknowledge Wei Wei Chi for initial help with the prototypes and testing. We also thank Mostafa Mirshekari for his initial thoughts about study design. We would like thank all our user study participants. This work was funded in part by the National Science Foundation under grant IIS-1718651.

REFERENCES

- [1] Nasa armstrong fact sheet: Fiber optic sensing system | nasa. <https://www.nasa.gov/centers/armstrong/news/FactSheets/FS-110-AFRC.html>. (Accessed on 02/09/2020).
- [2] Baam - big area additive manufacturing, 2019.
- [3] Boxzy home, 2019.
- [4] Objet30 pro desktop 3d printer for rapid prototyping, 2019.
- [5] Fiber Bragg Grating Manufacturing Workstation, Apr 2020. [Online; accessed 27. Apr. 2020].
- [6] Micron Optics, Apr 2020. [Online; accessed 27. Apr. 2020].
- [7] Farhad Ansari. *Sensing issues in civil structural health monitoring*. Springer, 2005.
- [8] Tyler J Arsenault, Ajit Achuthan, Pier Marzocca, Chiara Grappasonni, and Giuliano Coppotelli. Development of a fbg based distributed strain sensor system for wind turbine structural health monitoring. *Smart Materials and Structures*, 22(7):075027, 2013.
- [9] Amelie Bonde, Shijia Pan, Hae Young Noh, and Pei Zhang. Deskbuddy: an office activity detection system: demo abstract. In *Proceedings of the 18th International Conference on Information Processing in Sensor Networks*, pages 352–353, 2019.
- [10] Kristýna Čápková, Lukáš Velebil, and Jan Včelák. Laboratory and in-situ testing of integrated fbg sensors for shm for concrete and timber structures. *Sensors*, 20(6):1661, 2020.
- [11] A. J. Eronen, V. T. Peltonen, J. T. Tuomi, A. P. Klapuri, S. Fagerlund, T. Sorsa, G. Lorho, and J. Huopaniemi. Audio-based context recognition. *Trans. Audio, Speech and Lang. Proc.*, 14(1):321–329, December 2006.
- [12] J. Fagert, M. Mirshekari, S. Pan, P. Zhang, and H.Y. Noh. Characterizing left-right gait balance using footstep-induced structural vibrations. In *SPIE 10168, Sensors and Smart Structures Technologies for Civil, Mechanical, and Aerospace Systems*, volume 10168, pages 10168 – 10168 – 9, 2017.
- [13] James Fogarty, Carolyn Au, and Scott E. Hudson. Sensing from the basement: A feasibility study of unobtrusive and low-cost home activity recognition. In *Proceedings of the 19th Annual ACM Symposium on User Interface Software and Technology*, UIST '06, pages 91–100, New York, NY, USA, 2006. ACM.
- [14] Jon E. Froehlich, Eric Larson, Tim Campbell, Conor Haggerty, James Fogarty, and Shwetak N. Patel. Hydrosense: Infrastructure-mediated single-point sensing of whole-home water activity. In *Proceedings of the 11th International Conference on Ubiquitous Computing*, UbiComp '09, pages 235–244, New York, NY, USA, 2009. ACM.
- [15] Nan-Wei Gong, Steve Hodges, and Joseph A Paradiso. Leveraging conductive inkjet technology to build a scalable and versatile surface for ubiquitous sensing. In *Proceedings of the 13th international conference on Ubiquitous computing*, pages 45–54, 2011.

¹¹<https://www.digikey.com/products/en/tapes-adhesives-materials/glue-adhesives-applicators/909>

- [16] Anhong Guo, Anuraag Jain, Shomiron Ghose, Gierad Laput, Chris Harrison, and Jeffrey P. Bigham. Crowd-ai camera sensing in the real world. *Proc. ACM Interact. Mob. Wearable Ubiquitous Technol.*, 2(3):111:1–111:20, September 2018.
- [17] Daniele Inaudi. *Optical Fiber Sensors for Dam and Levee Monitoring and Damage Detection*, pages 91–120. 11 2019.
- [18] Daniele Inaudi and Branko Glisic. Long-Range Pipeline Monitoring by Distributed Fiber Optic Sensing. *American Society of Mechanical Engineers Digital Collection*, pages 763–772, Oct 2008.
- [19] Alexandra Ion, Johannes Frohnhofen, Ludwig Wall, Robert Kovacs, Mirela Alistar, Jack Lindsay, Pedro Lopes, Hsiang-Ting Chen, and Patrick Baudisch. Metamaterial mechanisms. In *Proceedings of the 29th Annual Symposium on User Interface Software and Technology*, UIST '16, pages 529–539, New York, NY, USA, 2016. ACM.
- [20] Alexandra Ion, Robert Kovacs, Oliver S. Schneider, Pedro Lopes, and Patrick Baudisch. Metamaterial textures. In *Proceedings of the 2018 CHI Conference on Human Factors in Computing Systems*, CHI '18, pages 336:1–336:12, New York, NY, USA, 2018. ACM.
- [21] Gayan Chanaka Kahandawa, Jayantha Ananda Epaarachchi, John Canning, Gang-Ding Peng, and Alan Lau. Development of embedded fbg sensor networks for shm systems. In *Structural Health Monitoring Technologies and Next-Generation Smart Composite Structures*, pages 61–88. CRC Press, 2016.
- [22] Cansu Karatas, Boray Degerliyurt, Yavuz Yaman, and Melin Sahin. Fibre bragg grating sensor applications for structural health monitoring. *Aircraft Engineering and Aerospace Technology*, 2018.
- [23] Raman Kashyap. *Fiber bragg gratings*. Academic press, Cambridge, MA, 2009.
- [24] JM Ko and YQ Ni. Technology developments in structural health monitoring of large-scale bridges. *Engineering structures*, 27(12):1715–1725, 2005.
- [25] Robert Kovacs, Alexandra Ion, Pedro Lopes, Tim Oesterreich, Johannes Filter, Philipp Otto, Tobias Arndt, Nico Ring, Melvin Witte, Anton Synytsia, and et al. Trussformer: 3d printing large kinetic structures. In *Proceedings of the 31st Annual ACM Symposium on User Interface Software and Technology*, UIST '18, pages 113–125, New York, NY, USA, 2018. Association for Computing Machinery.
- [26] Robert Kovacs, Anna Seufert, Ludwig Wall, Hsiang-Ting Chen, Florian Meinel, Willi Müller, Sijing You, Maximilian Brehm, Jonathan Striebel, Yannis Kommana, et al. Trussfab: Fabricating sturdy large-scale structures on desktop 3d printers. In *Proceedings of the 2017 CHI Conference on Human Factors in Computing Systems*, pages 2606–2616. ACM, 2017.
- [27] Benjamin Lafreniere, Tovi Grossman, Fraser Anderson, Justin Matejka, Heather Kerrick, Danil Nagy, Lauren Vasey, Evan Atherton, Nicholas Beirne, Marcelo H Coelho, et al. Crowdsourced fabrication. In *Proceedings of the 29th Annual Symposium on User Interface Software and Technology*, pages 15–28. ACM, 2016.
- [28] Gierad Laput, Karan Ahuja, Mayank Goel, and Chris Harrison. Ubicoustics: Plug-and-play acoustic activity recognition. In *Proceedings of the 31st Annual ACM Symposium on User Interface Software and Technology*, UIST '18, pages 213–224, New York, NY, USA, 2018. ACM.
- [29] Gierad Laput and Chris Harrison. Exploring the efficacy of sparse, general-purpose sensor constellations for wide-area activity sensing. *Proceedings of the ACM on Interactive, Mobile, Wearable and Ubiquitous Technologies*, 3(2):55, 2019.
- [30] Gierad Laput and Chris Harrison. Surfacesight: A new spin on touch, user, and object sensing for iot experiences. In *Proceedings of the 2019 CHI Conference on Human Factors in Computing Systems*, CHI '19, pages 329:1–329:12, New York, NY, USA, 2019. ACM.
- [31] Gierad Laput, Walter S. Lasecki, Jason Wiese, Robert Xiao, Jeffrey P. Bigham, and Chris Harrison. Sensors: Adaptive, rapidly deployable, human-intelligent sensor feeds. In *Proceedings of the 33rd Annual ACM Conference on Human Factors in Computing Systems*, CHI '15, pages 1935–1944, New York, NY, USA, 2015. ACM.
- [32] Gierad Laput, Yang Zhang, and Chris Harrison. Synthetic sensors: Towards general-purpose sensing. In *Proceedings of the 2017 CHI Conference on Human Factors in Computing Systems*, pages 3986–3999. ACM, 2017.
- [33] K. Loupos and A. Amditis. Structural Health Monitoring Fiber Optic Sensors. *SpringerLink*, pages 185–206, 2017.
- [34] Linjie Luo, Ilya Baran, Szymon Rusinkiewicz, and Wojciech Matusik. Chopper: partitioning models into 3d-printable parts. 2012.
- [35] R Maaskant, T Alavie, RM Measures, G Tadros, SH Rizkalla, and A Guha-Thakurta. Fiber-optic bragg grating sensors for bridge monitoring. *Cement and Concrete Composites*, 19(1):21–33, 1997.
- [36] Ramin Madarshahian, Juan M Caicedo, and Diego Arocha Zambrana. Benchmark problem for human activity identification using floor vibrations. *Expert Systems with Applications*, 62:263–272, 2016.
- [37] Micron Optics. *SM-130 Optical Sensing Interrogator*, 2009.
- [38] Mostafa Mirshekari, Jonathon Fagert, Shijia Pan, Pei Zhang, and Hae Young Noh. Step-level occupant detection across different structures through footstep-induced floor vibration using model transfer. *Journal of Engineering Mechanics*, 146(3):04019137, 2020.
- [39] Mostafa Mirshekari, Shijia Pan, Jonathon Fagert, Eve M Schooler, Pei Zhang, and Hae Young Noh. Occupant localization using footstep-induced structural vibration. *Mechanical Systems and Signal Processing*, 112:77–97, 2018.
- [40] Shijia Pan, Ceferino Gabriel Ramirez, Mostafa Mirshekari, Jonathon Fagert, Albert Jin Chung, Chih Chi Hu, John Paul Shen, Hae Young Noh, and Pei Zhang. Surfacevibe: Vibration-based tap & swipe tracking on ubiquitous surfaces. In *Proceedings of the 16th ACM/IEEE International Conference on Information Processing in Sensor Networks*, IPSN '17, pages 197–208, New York, NY, USA, 2017. ACM.
- [41] Shwetak N. Patel, Matthew S. Reynolds, and Gregory D. Abowd. Detecting human movement by differential air pressure sensing in hvac system ductwork: An exploration in infrastructure mediated sensing. In *Proceedings of the 6th International Conference on Pervasive Computing*, Pervasive '08, pages 1–18, Berlin, Heidelberg, 2008. Springer-Verlag.

- [42] Shwetak N. Patel, Thomas Robertson, Julie A. Kientz, Matthew S. Reynolds, and Gregory D. Abowd. At the flick of a switch: Detecting and classifying unique electrical events on the residential power line. In *Proceedings of the 9th International Conference on Ubiquitous Computing*, UbiComp '07, pages 271–288, Berlin, Heidelberg, 2007. Springer-Verlag.
- [43] PCB Piezotronics. *ICP Impact Hammer*, 2015.
- [44] Jeffrey D Poston, R Michael Buehrer, and Pablo A Tarazaga. A framework for occupancy tracking in a building via structural dynamics sensing of footstep vibrations. *Frontiers in Built Environment*, 3:65, 2017.
- [45] Nishkam Ravi, Nikhil Dandekar, Preetham Mysore, and Michael L Littman. Activity recognition from accelerometer data. In *Aaai*, volume 5, pages 1541–1546, 2005.
- [46] Bruce Richardson, Krispin Leydon, Mikael Fernstrom, and Joseph A Paradiso. Z-tiles: building blocks for modular, pressure-sensing floorspaces. In *CHI'04 extended abstracts on Human factors in computing systems*, pages 1529–1532, 2004.
- [47] Whitten L Schulz, Joel Pascal Conte, Eric Udd, and John M Seim. Static and dynamic testing of bridges and highways using long-gage fiber bragg grating based strain sensors. In *Industrial Sensing Systems*, volume 4202, pages 79–86. International Society for Optics and Photonics, 2000.
- [48] Erich P. Stuntebeck, Shwetak N. Patel, Thomas Robertson, Matthew S. Reynolds, and Gregory D. Abowd. Wideband powerline positioning for indoor localization. In *Proceedings of the 10th International Conference on Ubiquitous Computing*, UbiComp '08, pages 94–103, New York, NY, USA, 2008. ACM.
- [49] Saiganesh Swaminathan, Kadri Bugra Ozutemiz, Carmel Majidi, and Scott E. Hudson. Fiberwire: Embedding electronic function into 3d printed mechanically strong, lightweight carbon fiber composite objects. In *Proceedings of the 2019 CHI Conference on Human Factors in Computing Systems*, CHI '19, pages 567:1–567:11, New York, NY, USA, 2019. ACM.
- [50] Saiganesh Swaminathan, Michael Rivera, Runchang Kang, Zheng Luo, Kadri Bugra Ozutemiz, and Scott E Hudson. Input, output and construction methods for custom fabrication of room-scale deployable pneumatic structures. *Proceedings of the ACM on Interactive, Mobile, Wearable and Ubiquitous Technologies*, 3(2):62, 2019.
- [51] S Takeda, Y Aoki, T Ishikawa, N Takeda, and H Kikukawa. Structural health monitoring of composite wing structure during durability test. *Composite structures*, 79(1):133–139, 2007.
- [52] PM Toet, RAJ Hagen, HC Hakkesteegt, J Lugtenburg, and MP Maniscalco. Miniature and low cost fiber bragg grating interrogator for structural monitoring in nano-satellites. In *International Conference on Space Optics—ICSO 2014*, volume 10563, page 105631E. International Society for Optics and Photonics, 2017.
- [53] Karl Willis, Eric Brockmeyer, Scott Hudson, and Ivan Poupyrev. Printed optics: 3d printing of embedded optical elements for interactive devices. In *Proceedings of the 25th Annual ACM Symposium on User Interface Software and Technology*, UIST '12, pages 589–598, New York, NY, USA, 2012. ACM.
- [54] Hironori Yoshida, Takeo Igarashi, Yusuke Obuchi, Yosuke Takami, Jun Sato, Mika Araki, Masaaki Miki, Kosuke Nagata, Kazuhide Sakai, and Syunsuke Igarashi. Architecture-scale human-assisted additive manufacturing. *ACM Transactions on Graphics (TOG)*, 34(4):88, 2015.
- [55] Wei Zhang, Junqi Gao, Bin Shi, Heliang Cui, and Hong Zhu. Health monitoring of rehabilitated concrete bridges using distributed optical fiber sensing. *Computer-Aided Civil and Infrastructure Engineering*, 21(6):411–424, 2006.
- [56] Yang Zhang, Gierad Laput, and Chris Harrison. Vibrosight: Long-range vibrometry for smart environment sensing. In *The 31st Annual ACM Symposium on User Interface Software and Technology*, pages 225–236. ACM, 2018.
- [57] Yang Zhang, Chouchang Jack Yang, Scott E Hudson, Chris Harrison, and Alanson Sample. Wall++: Room-scale interactive and context-aware sensing. In *Proceedings of the 2018 CHI Conference on Human Factors in Computing Systems*, page 273. ACM, 2018.
- [58] Zhupeng Zheng and Ying Lei. Structural monitoring techniques for the largest excavation section subsea tunnel: Xiamen xiang’an subsea tunnel. *Journal of Aerospace Engineering*, 30(2):B4016002, 2017.
- [59] Jesus Zozaya. *Voltera: Build hardware faster*, 2019.